Proceedings of the 8th International Conference on Computing and Data Science
DOI: 10.54254/2755-2721/2026.38088

# *Virtual Inertia Deficiency and Control Optimization in High Renewable Penetration Power Systems*

**Kele Qian**

*Nanjing Normal University, Nanjing, China*
*kenqq2004@126.com*

***Abstract.*** High penetration of wind and photovoltaic generation is changing the frequency dynamic characteristics of modern power systems. When synchronous generators are replaced by inverter based resources, the equivalent system inertia decreases. After disturbances, frequency changes more rapidly, RoCoF increases, frequency nadir becomes lower, and recovery time becomes longer. This study focuses on virtual inertia deficiency and control optimization in high renewable penetration power systems. The IEEE 39 bus standard system is used to construct 0 percent, 30 percent, 50 percent, and 70 percent renewable penetration scenarios. MATPOWER, Python, and MATLAB/Simulink are combined for power flow calculation, controller parameter optimization, and time domain simulation. Three control strategies are compared, including no virtual inertia control, fixed parameter VSG control, and MPC optimized VSG control. The results show that when renewable penetration increases from 0 percent to 70 percent, equivalent inertia decreases from 4.85 s to 1.76 s, the maximum RoCoF increases from 0.31 Hz/s to 0.91 Hz/s, and the frequency nadir drops from 49.72 Hz to 49.43 Hz. MPC optimized control improves the frequency nadir to 49.61 Hz in the 70 percent renewable scenario and reduces storage power stress. These results indicate that virtual inertia allocation should be jointly optimized with renewable penetration, critical buses, and storage constraints. The framework provides a reproducible technical path for frequency security control in high renewable power systems.

***Keywords:*** virtual inertia, renewable energy, power systems, frequency stability, model predictive control

## 1. Introduction

Large-scale wind and photovoltaic integration is accelerating the transition of power systems toward clean energy and power-electronic interfaces. As synchronous generators are gradually displaced, system rotational inertia declines, causing faster frequency variations, higher RoCoF, lower frequency nadir, and longer recovery time after disturbances [1]. Existing studies have examined low-inertia frequency response, virtual synchronous control, and storage-assisted regulation, while many analyses still focus on individual controller behavior rather than the interaction between renewable penetration, inertia distribution, and system-level frequency security [2]. Against this background, the study focuses on virtual inertia deficiency and control optimization in high renewable penetration power systems. A standard benchmark system will be used to construct

© 2026 The Authors. This is an open access article distributed under the terms of the Creative Commons Attribution License 4.0 (https://creativecommons.org/licenses/by/4.0/).

DOI: 10.54254/2755-2721/2026.38088

multiple renewable penetration scenarios, while power-flow calculation, dynamic simulation, and parameter optimization will be combined to identify critical inertia-deficient locations and compare frequency stability under no control, fixed VSG control, and MPC-optimized control.

## 2. Literature review

### 2.1. Low-inertia frequency risk

The core source of low-inertia risk is the reduction of rotating kinetic energy after synchronous generators are replaced by converter-interfaced renewable units. When wind and photovoltaic generation is connected through inverters, its frequency support depends mainly on control algorithms rather than inherent mechanical inertia [3]. Frequency stability analysis therefore shifts from steady-state power balance to the fast dynamic process after disturbances, where RoCoF, frequency nadir, and recovery time become key indicators for evaluating frequency security [4]. Higher renewable penetration generally weakens initial frequency support, but the impact varies when different generator buses are replaced, indicating that inertia deficiency has clear spatial characteristics. By jointly considering renewable replacement level, disturbance location, and storage capacity constraints, the analysis can more accurately identify which areas require priority virtual inertia support and which operating conditions are more likely to trigger frequency instability.

### 2.2. Virtual Synchronous control logic

Virtual Synchronous Generator and Synchronverter control introduce inertia, damping, and droop characteristics similar to the swing equation of synchronous machines into inverter control loops, allowing power electronic devices to actively participate in frequency support [5]. These methods can rapidly adjust active power output during the early stage of a disturbance, raise the frequency nadir, and reduce RoCoF, making them common virtual inertia solutions in high renewable penetration systems [6]. Their performance is affected by the virtual inertia coefficient, damping coefficient, droop coefficient, and battery power limit. Small parameter values may provide insufficient support, while excessive values may increase active-power oscillation and storage stress. This means that virtual inertia control should move from single-device parameter tuning toward coordinated system-level optimization under multiple operating scenarios, especially when renewable penetration and disturbance intensity change simultaneously.

### 2.3. Intelligent scheduling pathways

With the development of computer-based optimization methods, MPC has gradually been applied to inverter power scheduling in low-inertia power systems because it can build a unified objective involving frequency deviation, power limits, SOC constraints, and recovery time [7]. Compared with fixed-parameter VSG control, MPC can dynamically adjust control actions according to renewable penetration level, disturbance intensity, and storage state, thereby improving adaptability across operating scenarios. MATPOWER can generate steady-state power-flow conditions for standard systems such as IEEE 39-bus, Python can support controller parameter optimization, and MATLAB/Simulink or PowerFactory can be used for time-domain dynamic simulation [8]. When virtual inertia sensitivity analysis and parameter boundary constraints are further included, the

DOI: 10.54254/2755-2721/2026.38088

optimization result can move beyond simple curve comparison and become an interpretable frequency security assessment with clearer engineering meaning [9].

## 3. Experimental methods

### 3.1. Public benchmark scenario design

The IEEE 39 bus New England standard system is used as the basic test case. The system includes 39 buses, 10 synchronous generators, and typical load buses. The case39 data are first loaded in MATPOWER to complete the baseline power flow calculation. Bus voltage magnitudes, voltage angles, generator active power output, and generator reactive power output are then obtained. After that, part of the synchronous generation is proportionally replaced by a combination of wind power, photovoltaic generation, and battery energy storage inverters. Renewable penetration scenarios of 30 percent, 50 percent, and 70 percent are constructed. Renewable replacement does not simply remove generator capacity. Instead, under the condition that total load and power balance are maintained, the original synchronous generator output is divided into equivalent renewable output and BESS regulation capacity. Wind power and photovoltaic generation are modeled as constant power grid connected units. The storage unit provides fast active power compensation. The disturbance is uniformly set as a 600 MW generator trip at 2 s. A 5 percent load step disturbance is also added. All scenarios use the same load level, disturbance time, and simulation duration. This ensures that the frequency response differences mainly come from renewable penetration, equivalent inertia reduction, and control strategy changes.

### 3.2. Controller parameter optimization

The control strategies are divided into three groups. The first group has no virtual inertia control and only retains the governor response of the original synchronous machines. The second group adopts fixed parameter VSG control. All renewable inverters use the same virtual inertia and damping parameters. The third group adopts MPC optimized VSG control. The control parameters are dynamically adjusted according to renewable penetration and disturbance intensity [10]. The core of VSG is to make the active power output of the inverter simulate the swing process of a synchronous machine, as shown in Formula 1.

$$2H_v \frac{d\Delta\omega}{dt} = P_{ref} - P_{inv} - D_v \Delta\omega \tag{1}$$

Here, $H_v$ denotes the virtual inertia coefficient. $\Delta\omega$ denotes the angular frequency deviation. $P_{ref}$ denotes the inverter reference power. $P_{inv}$ denotes the actual inverter output power. $D_v$ denotes the virtual damping coefficient. The active power compensation of the inverter is jointly determined by frequency deviation and frequency change rate, as shown in Formula 2.

$$\Delta P_{inv} = K_f (f_0 - f) + K_r \frac{df}{dt} \tag{2}$$

Here, $\Delta P_{inv}$ denotes the active power regulation of the inverter. $K_f$ denotes the frequency droop coefficient. $K_r$ denotes the inertia response coefficient. $f_0$ denotes the nominal frequency. f denotes

DOI: 10.54254/2755-2721/2026.38088

the real time system frequency. The MPC optimization aims to reduce frequency deviation, suppress RoCoF, and control storage power fluctuation, as shown in Formula 3.

$$\min J=\sum_{k=1}^{N}\left(q_1\Delta f_k^2+q_2 RoCoF_k^2+q_3\Delta P_{b,k}^2+q_4\Delta SOC_k^2\right) \tag{3}$$

Here, J denotes the objective function. N denotes the prediction horizon. $\Delta f_k$ denotes the frequency deviation at step k. $\Delta P_{b,k}$ denotes the change in storage power. $\Delta SOC_k$ denotes the change in the battery state of charge. $q_1$ to $q_4$ denote the weighting coefficients. The optimization problem is solved by cvxpy in Python. The constraints include the storage power limit, SOC range, inverter ramp rate, and frequency security boundary. The optimized parameters are then imported into the Simulink control module for dynamic simulation.

### 3.3. Time-domain evaluation workflow

The time domain simulation follows the sequence of power flow initialization, dynamic disturbance, control response, and indicator calculation. MATPOWER first outputs the stable power flow results. Bus voltage, generator output, and load parameters are used as the initial values of the Simulink dynamic model. The synchronous machine, governor, inverter, VSG controller, MPC controller, and BESS modules are then built in Simulink. The total simulation time is set to 20 s. The sampling step is set to 0.01 s. The disturbance is triggered at 2 s. Each simulation records the system center frequency, key bus voltage, inverter active power output, storage SOC, and control power change [11]. RoCoF is used to measure the initial frequency change speed after the disturbance, as shown in Formula 4.

$$RoCoF(t)=\frac{f(t)-f(t-\Delta t)}{\Delta t} \tag{4}$$

Here, $RoCoF(t)$ denotes the rate of change of frequency at time t. f(t) and f(t−Δt) denote the current frequency and the frequency at the previous sampling point, respectively. Δt denotes the sampling interval. The comprehensive frequency stability cost is used to compare the overall performance of different control strategies, as shown in Formula 5.

$$C=\alpha|RoCoF|_{max}+\beta\left(f_0-f_{min}\right)+\gamma T_s+\lambda E_b \tag{5}$$

Here, C denotes the comprehensive stability cost. $|RoCoF|_{max}$ denotes the maximum rate of change of frequency. $f_{min}$ denotes the frequency nadir. $T_s$ denotes the frequency recovery time. $E_b$ denotes the storage energy consumption. α, β, γ, and λ denote the evaluation weights. This workflow can directly compare inertia deficiency under different renewable penetration levels. It can also test the improvement of fixed VSG and MPC optimized VSG in frequency security, storage stress, and recovery speed.

DOI: 10.54254/2755-2721/2026.38088

# 4. Results

## 4.1. Inertia deficiency identification results

As shown in Table 1, under the same 600 MW generator tripping disturbance, the increase in renewable penetration leads to a continuous decline in equivalent inertia, a larger absolute RoCoF, a lower frequency nadir, and a longer recovery time. This indicates that after synchronous generators are replaced by inverter based resources, the initial frequency support capacity of the system is clearly weakened. In the baseline scenario, the equivalent inertia is 4.85 s, the maximum RoCoF is 0.31 Hz/s, and the frequency nadir is 49.72 Hz. When renewable penetration increases to 70 percent, the equivalent inertia drops to 1.76 s, the maximum RoCoF rises to 0.91 Hz/s, the frequency nadir decreases to 49.43 Hz, and the recovery time extends to 12.8 s. This set of data corresponds to the scenario construction in Section 3.1. It shows that high renewable replacement changes the generation structure and directly reshapes the dynamic security boundary of the system. The deeper frequency drop after replacing key generator buses indicates that virtual inertia should be preferentially allocated to nodes with higher inertia contribution.

Table 1. Frequency stability indicators under different renewable penetration levels

| Scenario | Renewable Penetration | Equivalent Inertia Hsys/s | Maximum RoCoF/Hz·s$^{-1}$ | Frequency Nadir/Hz | Recovery Time/s |
|---|---|---|---|---|---|
| S0 | 0% | 4.85 | 0.31 | 49.72 | 6.4 |
| S1 | 30% | 3.52 | 0.46 | 49.63 | 8.1 |
| S2 | 50% | 2.48 | 0.68 | 49.54 | 10.3 |
| S3 | 70% | 1.76 | 0.91 | 49.43 | 12.8 |

## 4.2. Optimized control performance results

As shown in Figure 1, the frequency nadir is jointly affected by renewable penetration and the virtual inertia coefficient. From the horizontal direction, when renewable penetration increases from 30 percent to 70 percent, the overall frequency nadir decreases. This indicates that inertia deficiency becomes more severe as the replacement ratio increases. From the vertical direction, when $H_v$ increases from 2 s to 6 s, the frequency nadir gradually rises. In the 70 percent renewable scenario, it improves from 49.43 Hz to 49.61 Hz, showing that virtual inertia can reduce the depth of the initial frequency drop after disturbance. When $H_v$ further increases to 8 s, the improvement becomes limited. A slight decline appears in some scenarios. This suggests that excessive virtual inertia may increase the instantaneous power pressure on BESS and introduce control delay. Combined with the MPC objective function in Section 3.2, the relatively optimal parameter range is concentrated around $H_v$=5~6s. Within this range, frequency security, storage power demand, and recovery speed can reach a better balance.

DOI: 10.54254/2755-2721/2026.38088

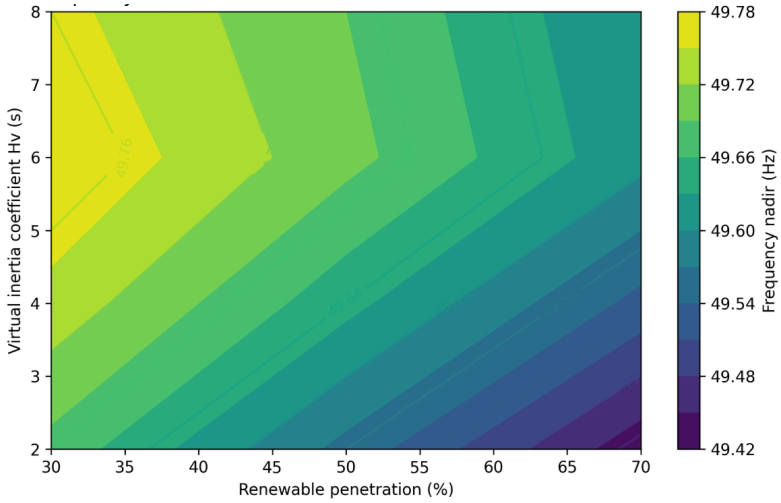



Figure 1. Contour map of frequency nadir under different renewable penetration levels and virtual inertia coefficients

## 5. Discussion

The experimental results show that frequency risk does not increase in a purely linear way with renewable penetration. As the proportion of synchronous generation declines, the system becomes more dynamically sensitive to disturbances. In the 50 percent and 70 percent scenarios, the obvious increase in RoCoF indicates that the system lacks sufficient fast power support during the initial disturbance stage. After synchronous inertia is replaced, the frequency security boundary becomes narrower. Fixed parameter VSG improves the frequency nadir, but its performance is limited by virtual inertia and damping settings. In high renewable scenarios, it may also cause active power fluctuation. MPC optimized VSG shows more stable performance because it considers frequency deviation, RoCoF, storage power, and SOC constraints at the same time. The virtual inertia coefficient performs better around 5 to 6 s. Excessive virtual inertia increases the instantaneous output pressure of BESS and may delay the frequency recovery process.

## 6. Conclusion

A simulation framework is established to study virtual inertia deficiency and control optimization in high renewable penetration power systems based on the IEEE 39 bus benchmark. The research process first uses MATPOWER for power flow initialization. Then synchronous machines, inverters, VSG, MPC, and BESS dynamic models are built in MATLAB/Simulink. Python is used for controller parameter optimization. The experimental results show that as renewable penetration increases, equivalent system inertia continues to decline, RoCoF increases, frequency nadir decreases, and recovery time becomes longer. Fixed parameter VSG can provide inertia support, but its adaptability is limited under multiple operating scenarios. MPC optimized VSG achieves a better balance between frequency stability and storage constraints. Overall, the combination of power system dynamic simulation and computer based optimization provides a feasible solution for frequency security analysis and virtual inertia allocation in clean power systems.

DOI: 10.54254/2755-2721/2026.38088

## References


[1] Ahmed, F., et al. (2023). Dynamic grid stability in low carbon power systems with minimum inertia. *Renewable Energy, 210*, 486–506.

[2] Shakerighadi, B., et al. (2023). An overview of stability challenges for power-electronic-dominated power systems: The grid-forming approach. *IET Generation, Transmission & Distribution, 17*(2), 284–306.

[3] Gotti, D., Ledesma, P., & Amaris, H. (2023). A recursive system identification inertia estimator for traditional and converter-interfaced generators. *International Journal of Electrical Power & Energy Systems, 154*, 109445.

[4] Oshnoei, S., et al. (2023). A novel virtual inertia control strategy for frequency regulation of islanded microgrid using two-layer multiple model predictive control. *Applied Energy, 343*, 121233.

[5] Bakeer, M., et al. (2023). Resilient virtual synchronous generator approach using DC-link capacitor energy for frequency support of interconnected renewable power systems. *Journal of Energy Storage, 65*, 107230.

[6] Elwakil, M. M., et al. (2023). Adaptive virtual synchronous generator control using optimized bang-bang for islanded microgrid stability improvement. *Protection & Control of Modern Power Systems, 8*(1).

[7] Maleki, S., Nikoukar, J., & Tousifian, M. H. (2023). Robust frequency control of microgrids: A mixed H 2/H∞ virtual inertia emulation. *International Transactions on Electrical Energy Systems, 2023*(1), 6872765.

[8] Hosseini, S. A. (2024). Frequency control using electric vehicles with adaptive latency compensation and variable speed wind turbines using modified virtual inertia controller. *International Journal of Electrical Power & Energy Systems, 155*, 109535.

[9] Sati, S. E., et al. (2024). A novel virtual inertia-based damping stabilizer for frequency control enhancement for islanded microgrid. *International Journal of Electrical Power & Energy Systems, 155*, 109580.

[10] Saleem, M. I., & Saha, S. (2024). Assessment of frequency stability and required inertial support for power grids with high penetration of renewable energy sources. *Electric Power Systems Research, 229*, 110184.

[11] Jafari, M., Gharehpetian, G. B., & Anvari-Moghaddam, A. (2024). On the role of virtual inertia units in modern power systems: A review of control strategies, applications and recent developments. *International Journal of Electrical Power & Energy Systems, 159*, 110067.